Investigation of Force-Sensor-Integrated Motorized Spindles and Diagnosis of Unbalanced Tool Operation

Yi-Lin He
Buffalo Machinery CO., LTD.,
Taichung City, Taiwan
r47@mail.buffalo.com.tw

Hsun-Fu Chiang
Buffalo Machinery CO., LTD.,
Taichung City, Taiwan
r43@mail.buffalo.com.tw

Paul Chang
Buffalo Machinery CO., LTD.,
Taichung City, Taiwan
paulchang@mail.buffalo.com.tw

2022 International Conference on Applied Electronics (AE) | 978-1-6654-9482-3/22/$31.00 ©2022 IEEE | DOI: 10.1109/AE54730.2022.9920035

***Abstract*—The motorized spindles play an important role in high precision and high speed metal cutting, and increase productivity benefit in die and mode, medical, and aerospace industries. As a result, improper high speed operation of bearings and system causes lower reliability. Lot of technology and sensors are development to monitor the failure of improper operation of motorized spindle. In this paper, one piezo-electric force sensor is developed. And, One Class SVM is investigated to monitoring and detects the unbalanced tool operation. The result shows the monitoring system is validated successfully.**

Keywords—piezo-electric force sensor, motorized spindle, diagnosis, One Class SVM

I. Introduction

The industrie 4.0 are introduced in 2013 from Germany to enhance the productivity [1]. The one of the production enhancement is to reduce machine down time, therefore the machine diagnosis and fault detection play an important role in industrie 4.0 production line.

In the machine tool industry, the high-speed motorized spindle increases the productivity. The main spindle can be operated in speed range from 18,000 rpm to 200,000 rpm, is dependent on the application requirement and state-of-art of bearing. The ultra-precision angle contact bearing is commonly applied in high-speed motorized spindle. The spindle service time is limited by the bearing preload, lubrication, undesired vibration load, [2] which induces additional force on the bearings, and undesired mechanical-resonance force. For example, the tool insert is broken during machining will cause large centrifugal force.

The papers study the force-sensor based mechanical design to be applied in the high speed motorized spindle [3],[4]. This paper presents force-sensor-integrated spindle to measure cutting force, and a dynamically compensated sensor system with Kalman Filter. The filter is designed to filter the influence of structural modes on the force sensor, since sensor output contains the structure vibration of spindles. In addition, the bandwidth of the force sensing system is improved as well [4]. These papers focus the force measurement application from the tool tip and signal compensation.

In this paper, the force-sensor-integrated motorized spindle is developed, including the force sensor ring and signal conditioner. And, the diagnosis of unbalanced tool is investigated with PCA and on-class SVM for the force ring system.

II. System Block Diagram

The Fig. 1 shows the system block diagram; there is a force sensor inside spindle. Since the force sensor is located in the force links, the high-stiffness piezo material sensor is selected as the force measurement device. The charge amplifier is designed for the signal conditioning device. The PC is the acquiring device and software platform for program of diagnosis. The high-speed sampling DAQ card is adopted in PC for the signal transformation device. The diagnosis will be illustrated in section IV.

The electric signal from the piezo-electric sensors are fed to the charge amplifiers. Then, algorithm is developed to analysis the abnormal signal. The core algorithm is novelty detection, which will be illustrated in Section IV.

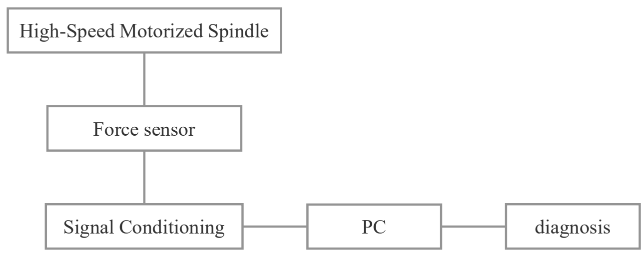

Fig. 1 System Block Diagram

A. The Motorized Spindle with Force Sensor Ring

A real-time monitoring device is required for the high-speed spindle to ensure any abnormal bearings revolution conditions could be detected. Some solutions have considered placing a vibration unit outside the spindle, and although this works, it is sensitivity to detect the force from tool side. The operator may need to be aware of the abnormal bearing motion conditions. A direct monitoring unit placed in front of the bearing is proposed as shown in Fig. 2.(a) The various bearing arrangement could be chosen for different application, according to the requirement of bearing service time and stiffness. In this study, the tandem bearing arrangement is applied to keep the cost effective and better cutting performance. To maximize the sensitivity of the force to the signal from the piezo-element, the force sensor is installed between the front bearing #1 and front bearing #2.

The simplified assembly drawing is shown in Fig. 2.(b) and Fig. 2.(c), and Mark A is the spindle bearing and sensor ring assembly, and Mark B is the sensor inserted into the space ring, as indicated in Fig. 2.(c). There are four sensors at every 90 degrees, which can monitor any abnormal bearing motion, and both sides of the spacer ring are

978-1-6654-9482-3/22/$31.00 ©2022 IEEE

provided with four sensors, which allow both bearings to be monitored whenever the spindle is rotating. When the pressure to the sensor is out of balance, the sensor obtains different data to that while the bearing outer ring is out of balance, which enables the sensor and amplifiers to be activated and a real-time monitoring to take place.

Fig. 2.(c) shows all the applied components, whereas the mark B indicates the location piezo-electric sensor element, which is a highly sensitive. The FS ring is composed by four piezo-electric elements and four dummies. The dummies are placed between any two sensors by 45 degree. The sensitivity is -4 pC/N, with 4 pcs placed at every 90 degrees of the ring, and both sides of the rings are provided with the same unit to enable a real-time monitoring function. The mark B is the sensor and the mark C is the holding ring placed between both angular contact bearings, while the holding ring is also applied as a spacer.

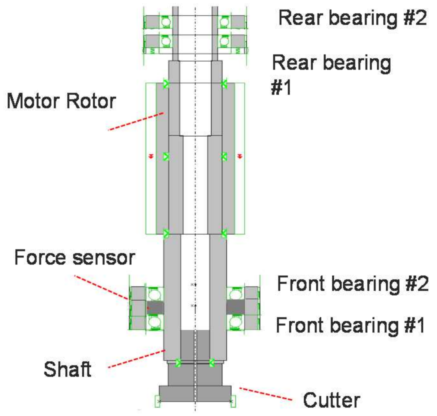

(a) The whole spindle geometric with front and rear bearings

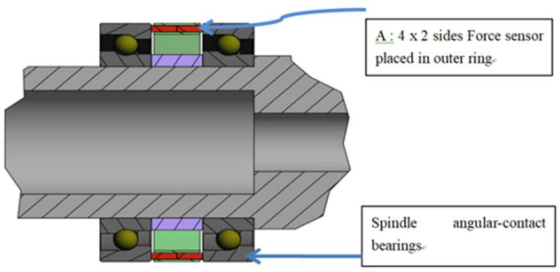

(b) spindle bearings with force sensor assembly (simplified drawing)

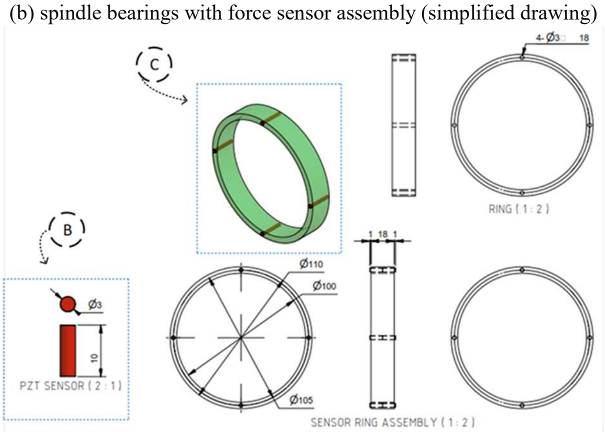

(c) Holding ring and sensor (simplified drawing)

Fig. 2 The illustration of high-speed motorized spindle and the force sensor photograph. Source of figures is from Department of Research and Develope, Buffalo Machinery co. ltd.

B. Characteristic of Piezo Electrical Sensor

From the industrial experience, the operation temperature of spindle bearing is usually under 50 ℃, which is dependent on the spindle manufacturer, due to the spindle design, material of bearing cage, cooling, and the lubrication condition. This can be finding from the spindle manual. On the other hand, the bearing operation temperature is limited by the retainers, which is made up by phenolic are used at operating temperatures up to 270 °F(132 ℃). Consequently, for all the sensors, the maximum operation temperature of 120 ℃ could reasonably cover the operation temperature. The TABLE I shows the key parameter of piezo-electric sensor element. For each sensor, the sensitivity, linearity, and hysteresis are listed in TABLE II.

The sensor ring output characteristics, relationship of the generated charge and force are measured by tensile testing machine, the proposed force sensor ring is assembly to the tensile testing machine with a suitable jig. The measure result is shows in Fig. 3. Since there are eight force link paths in the sensor ring, the sign is neglected, the sensitivity is close to 0.5 pC/N, it is calculated by 6000 pC of output charge divide 12 kN of maximum testing force. This is close to the theoretical value.

TABLE I THE PARAMETER OF PIEZO ELECTRIC SENSOR

***Sensitivity* [pC/N]**	-4 pC/N
Measurable normal force, F_N [N]	3 kN
Sensor operation temperature [℃]	-20 ~ 120
Sensor storage temperature [℃]	-20 ~ 120
Fundamental resonance frequency [Hz]	120

TABLE II THE SENSITIVITY OF PIEZO ELECTRIC SENSOR

Position	***Sensitivity [pC/N]***	***Linearity [%FSO]***	***Hysteresis [%FSO]***
#1	4.026	0.443	0.388
#2	3.998	0.539	0.335
#3	3.960	0.518	0.332
#4	4.074	0.455	0.253

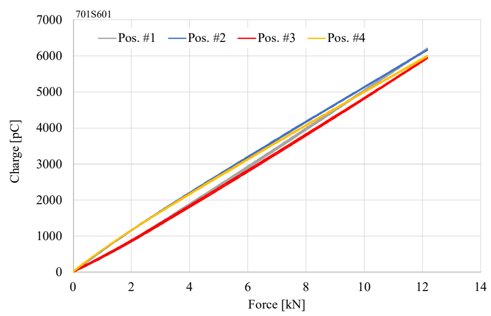

Fig. 3 The output characteristic of piezo-electric sensors.

C. The Signal Conditioner

The signal conditioner is shown in Fig. 4. Based on the charge output characteristic of piezo-electric sensor, the 1st stage is the charge amplifier, which transfers the charge signal into voltage for analysis. The low-3dB frequency is decided by equation (1) [5]. The charge amplifier works like a high pass filter respect to the charge, Qi. The output stage is the invert voltage amplifier with low pass filter. The higher-3dB frequency is decided by equation (2), i.e. the C3 and R4. And, according to the diagnosis application, the frequency range of interesting signal must be in the range of lowe-3dB frequency and high-3dB frequency.

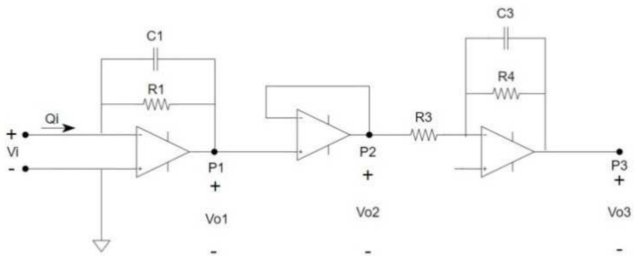

Fig. 4 The simplified circuit diagram of signal conditioner. The first stage is charge amplifier, 2nd stage is voltage follower, and the final stage is invert amplifier.

$$f_{LOW,3dB} = \frac{1}{2\pi R_1 C_1} \quad (1)$$

$$f_{HIGH,3dB} = \frac{1}{2\pi R_4 C_3} \quad (2)$$

To decide the 3dB frequency, common frequency appears in spindle and bearings are evaluated, as shown in TABLE III. The failure bearings frequency is discussed in[6],[7]. In this paper, the max speed of spindle is 20,000 rpm, this gives the maximum shaft frequency. The ballpass frequency of inner race decides the maximum frequency in the mechanical system, i.e. 7.49 kHz. Therefore, the high-3dB frequency of 20kHz is chosen. The circuit parameters are listed in TABLE IV. Notably, the practical high-3dB frequency is slightly higher than the designed values, due to the 47pF closest values can be find. The Fig. 5 shows that the Bode plot, three C1 capacitances are tested for comparison. As shown in Fig. 5, the $f_{HIGH,3dB}$ and $f_{LOW,3dB}$ are close to the theorem calculation values.

TABLE III. THE POSSIBLE APPEAR FREQUENCY IN THE SPINDLE AND BEARINGS. THE f_r IS THE SHAFT SPEED, THE N IS THE NUMBER OF ROLLING, ϕ IS THE ANGLE OF THE LOAD FROM THE RADIAL PLANE. WHEREAS THE D=14.2MM, D=110, N=20, ϕ=15∘, THE 7016-BEARING WITH 15∘ IS ADOPTED IN THE SPINDLE[8].

Item	frequency [Hz]
Shaft frequency for 20,000 rpm spindle, f_r	0.67k
Cutting frequency for 5 cuts tool and 20,000 rpm	3.33k
BPFO($=\frac{nf_r}{2}\left\{1-\frac{d}{D}cos\phi\right\}$)	5.82k
BPFI($=\frac{nf_r}{2}\left\{1+\frac{d}{D}cos\phi\right\}$)	7.49k
FTF($=\frac{f_r}{2}\left\{1-\frac{d}{D}cos\phi\right\}$)	291
BSF($=\frac{D}{2d}\left\{1-\left(\frac{d}{D}cos\phi\right)^2\right\}$)	0.905

TABLE IV THE CIRCUIT PARAMETERS

item	values
$f_{LOW,3dB}$	26.5 mHz
$f_{HIGH,3dB}$	Design 20 kHz (practical 22.5 kHz)
C1	1 nF
R1	3 GΩ
R3	6.8kΩ
R4	150 kΩ
C3	47 pF

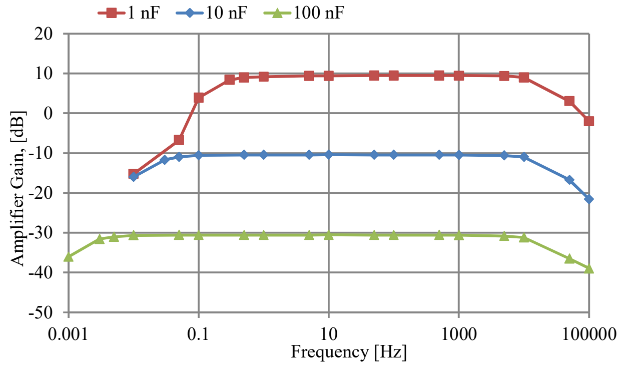

Fig. 5 The Bode plot diagram – serval RC time-constant testing for the implemented charge amplifier

III. MEASUREMENT CAMPAIN FEATURE EXTRACTION, AND PREPARATION SAMPLES

One accelerometer is mounted on the spindle for vibration reference. The ISO 17243 suggests the accelerometer should be close to the bearing as much as possible. The vibration meter, G-TECH vPOD, is applied in this experiment to measure the vibration level. All time domain data will be transferred in frequency domain via Fast Fourier Transform.

A. The Consideration of Vibration Magnitude and Definition the Positive/negative Samples

The bearing fault diagnosis of machine tool spindle is based on the ISO 17243-1 [9]. There ISO 17243-1 suggests one accelerometer is mounted on spindle to measure the vibration. The standard of ISO 17243 suggest that, the vibration magnitude of 0.7 mm/s is good vibration level for a ball bearing spindle and power is higher than 5kW, as shown in TABLE V. In this paper, the vibration magnitude is lower than 0.4 mm/s is selected for positive samples. Otherwise, the negative samples are.

TABLE V. THE VIBRATION MAGNITUDE REFERENCE GUIDE FOR MACHINE TOOL SPINDLE

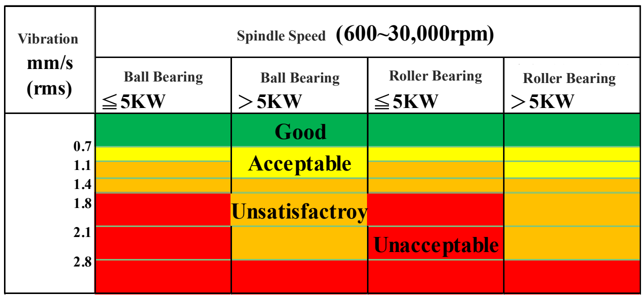

B. Experiment setup for Unbalanced Cutter

a) Measure Campaign and Result.

A HSK-A63 tool with eight inserts is selected as the target cutter. As shown in Fig. 6, the photographs show one normal cutter setup and two abnormal cutter setups. To prevent the irreversible damage occurs to the motorized spindle, only maximum speed of 4,000 rpm is tested in this experiment. The 4,000 rpm speed is tested, therefore, the fundamental frequency, fz, is 66.6 Hz, the second harmonics frequency, f2, is 133.3 Hz. The Fig. 7 shows the spindle vibration result. The normal cutter gives the lowest vibration values, once the any insert is removed, the balance statement is broken.

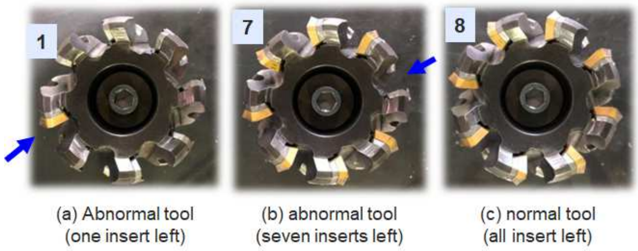

Fig. 6. the cutter for three different experiment setup

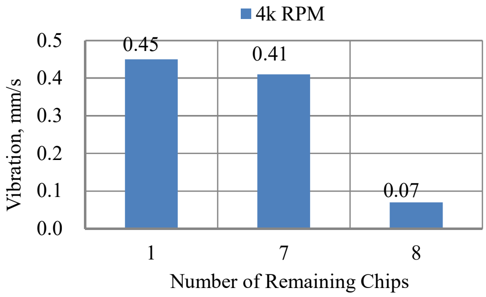

Fig. 7. The experiment result of the unbalanced tool

b) Feature Evaluation by the Spectrum

The time domain and frequency domain signal are shown in Fig. 8. It shows clearly that the fundamental frequency of spindle is 66.6 Hz, while the spindle is operated in 4,000 rpm. The magnitude of fundamental frequency and 2^{nd} harmonic is in the range of - 40dB ~ - 50dB. The 3rd and 4th harmonic could be seen slightly. And, the higher harmonics cannot be recognized well.

The FFT result of three kinds of inserts are shown in Fig. 9a. The magnitude of fundamental frequency is sensitivity to the inserts number, since the insert decides the balance of rotating shaft. The other harmonics are not changed significantly. As a result, by this experiment data, the components of fundamental frequency are selected as features for the diagnosis model investigation

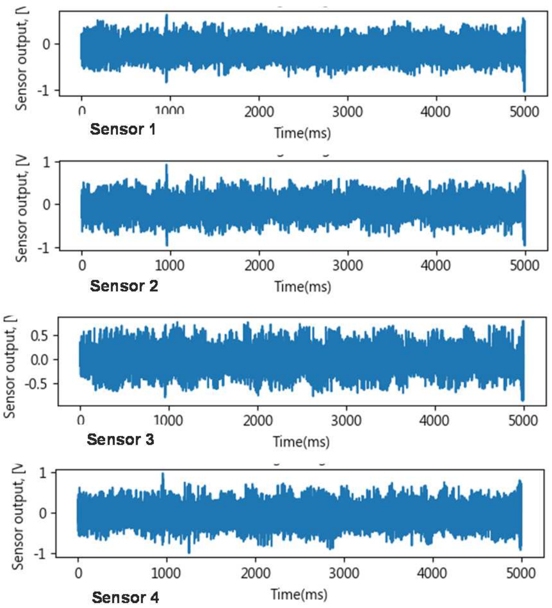

(a) Waveforms in time domain

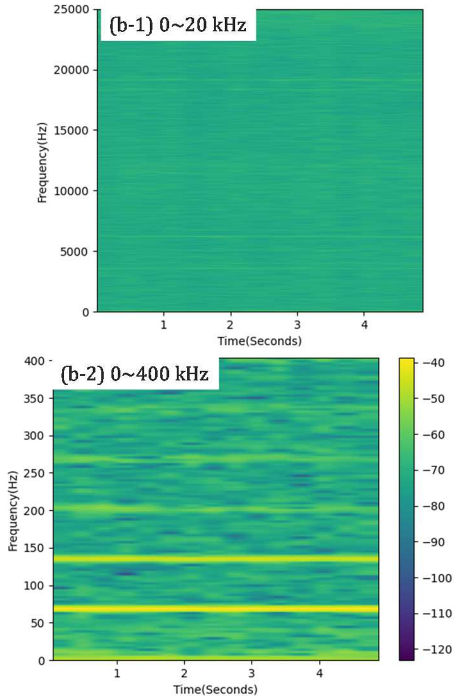

(b) Spectrogram of sensor 1,
only show one of the time period in 5 seconds

Fig. 8. An example of the acquired vibration signal

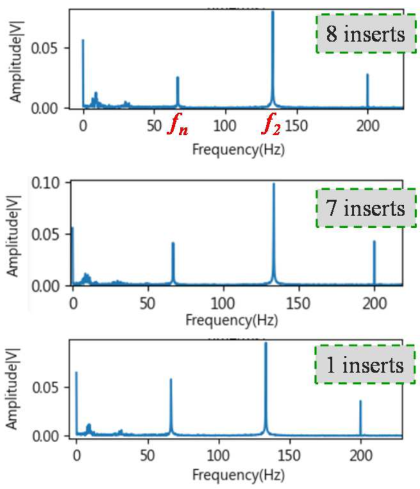

Fig. 9. The FFT comparison of acquired vibration signal.

IV. The Investigation of the OCSVM for Diagnosis of Unbalanced Cutter

A. Flowchart

Firstly, there are four frequency signals from the force sensor, as the four features for PCA. The principal components are extracted by the PCA technique. In this paper, there are four features and four principal components will be obtained. The features and principal components could be linearly transformed each other. The high variance ratios of principal components are chosen as the training-model data for the one-class SVM.

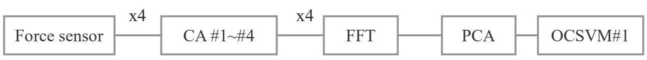

Fig. 10. The block diagram of the algorithm

B. *Principal components analysis, PCA*

The Principal component analysis (PCA) is the process for computing the principal components. The PCA is one of the techniques of dimensionality reduction for saving the data memory. In the meantime, it keeps the maximum covariance of data by select the first few principle components.

C. *One-Class Support Vector Machine*

The mechanical vibration (i.e. the signal from the force sensor) is not fully defined in this paper, it means that may be there are much unexplored data. Only the normal operation data and few pre-defined abnormal operation data can be obtained. As a result, one or multi- simple boundary are not easy to be defined. In this study, one-class support vector machine is used for novelty detection [10].

In this paper, only normal operation data and few pre-defined abnormal operation data can be obtained. The one-class SVM algorithm, which is not similar to regular SVM, cannot maximize the margin between two classes [11]. Alternatively, the target of algorithm of the one-class SVM is to find a small region (usually the positive data) to cover all positive data as much as possible. The data are out of the region that represent faulty region. To find a proper region for separating the data, the data are map into feature space by a known kernel function.

The kernel selection is importance, as kernel decides the algorithm performance, is dependent on the data and the number of features [12]. In this paper, the Gaussian radial base function (RBF) is selected.

V. Result and Discussion

The key values of PCA are shown in TABLE VI. The Variance ratio of 1st principal component is 0.8203, the 2nd one is 0.1591. So, the first two components are selected for the model data.

The result of training model for one-class SVM is shown in Fig. 11. Notably, as aforementioned, there are two features be extracted from the four signals of force sensor. All drawing data are transformed to the new space, which is obtained from the PCA and composed by the 1st principal component and 2nd principal component.

As shown in Fig. 11, the abnormal data sets are clearly far away from the normal data set. The case of one-insert tool locates in the right-hand side. Similar to the Fig. 9 shown, the magnitude of one-insert tool is the highest values. The model accuracy of one-class SVM is obtained by varying the γ and ν parameters. The best accuracy for parameters γ=5 and ν =0.001 is 99.7 %. The result shows the feasibility of this study. In the case of broken inserts and lose inserts, the investigated model is able to detect.

TABLE VI. The key values of PCA

Component	Singular Values	Variance ratio
1st	3.02621	0.8203
2nd	1.33294	0.1591
3rd	0.36539	0.0120
4th	0.30939	0.0086

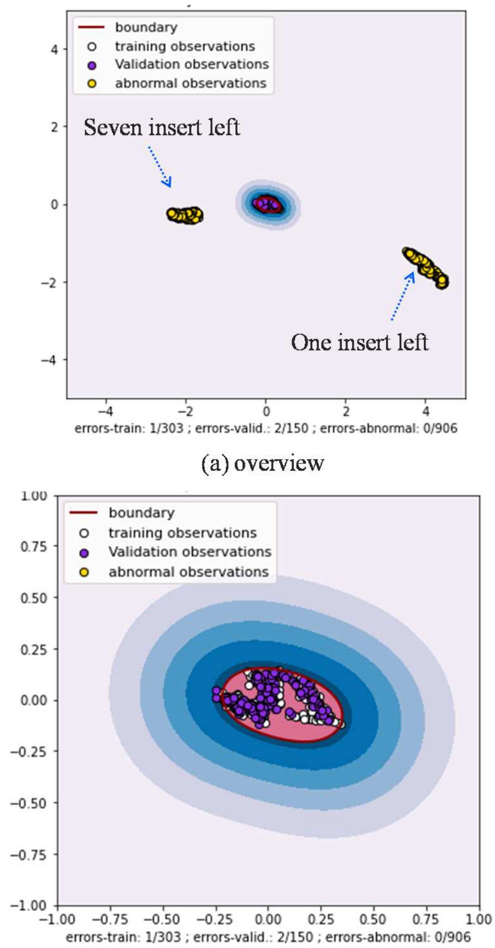

(b) ν =0.001, γ=5, accuracy = 99.7% (301/303)

Fig. 11. The scatter plot of the analysis result.

VI. Conclusion

The present study validates the force sensor and the AI-based monitoring system. Firstly, the force sensor is sensitivity to the centrifugal force induced from the unbalanced tool. Secondly, the unbalanced tool operation could be detected by using the One-Class SVM for a given operation and the data set. The force-sensor-based mechatronics application and AI-based monitoring system gives another approach of abnormal detection for spindle/bearing.

Acknowledgment

The authors would like to thank professors and all colleagues who contributed to this study. My thanks go to Professor Yi-Hung Liu of mechanical engineering at National Taiwan University of Science and Technology for advising and algorithm expertise. The authors wish to acknowledge the Professor Shih-Ying Chang of mechanical engineering at National Yunlin University of Science and Technology and Professor Bo-Chiuan Chen of National Taipei University of Technology in invaluable comment. The authors would like to thank Chien-Hang Chan and Ku-An Tu who support the experiment assistance and data recording of the experiment. The authors would like to thank Yik-Ai Wu and Hao-Yun Chiang who develop the code for algorithm.

REFERENCES

[1] Henning Kagermann, “Recommendation for Implementing the Strategy Initiative Industries 4.0,” Communication Promoters Group of the Industry-Science Research Alliance, National Academy of Science and Engineering, Apr. 2013.

[2] Li Cui, “A new fatigue damage accumulation rating life model of ball bearings under vibration load,” Industrial Lubrication and Tribology, Vol. 72, Iss. 10, pp. 1205-1215, 2020.

[3] Simon S. Park and Yusuf Altintas, “Dynamic Compensation of Cutting Forces Measured from the Spindle Integrated Force Sensor System,” Proceedings of IMECE2002, 2002.

[4] Simon S. Park and Yusuf Altintas, “Dynamic Compensation of spindle integrated force sensors with Kalman Filter,” Journal of Dynamic Systems, Measurement, and Control , vol. 126, pp. 443-254, 2004.

[5] Dan Mihai Ştefănescu, *Handbook of Force Transducers Principles and Components*, p. 123, ISBN: 978-3-642-18296-9.

[6] Robert B. Randall and Je´rome Antoni, “Rolling element bearing diagnostics—A tutorial,” Vol. 25, Iss. 2, pp. 485-520, Feb. 2011

[7] R. Serrato, M.M. Maru, and L.R. Padovese, “Effect of Lubricant viscosity grade on mechanical vibration of roller bearings, Tribology International, Vol. 40, pp. 1270-1275, 2007.

[8] Datasheet of Super Precision Angular contact ball bearings, 7016 CD, elink: https://www. skf.com/uk/products/super-precision-bearings /angular-contact-ball-bearings/productid-7016%20CD%2FHCP4A

[9] ISO/TR 17243-2:2017, Machine tool spindles — Evaluation of spindle vibrations by measurements on non-rotating parts — Part 2: Direct-driven spindles and belt-driven spindles with rolling element bearings operating at speeds between 600 r/min and 30 000 r/min.

[10] Juhamatti Saari, Daniel Strömbergsson, Jan Lundberg, and Allan Thomson, “Detection and identification of windmill bearing faults using a one-class support vector machine (SVM), measurement, vol. 137, pp. 287-301, 2019

[11] B. Schölkopf, R.C. Williamson, A.J. Smola, J. Shawe-Taylor, J.C. Platt, et al, “Support vector method for novelty detection,” NIPS, Vol. 12, pp 582–588, 1999.

[12] K.-R. Muller, S. Mika, G. Ratsch, K. Tsuda, and B. Scholkopf, “An introduction to kernel-based learning algorithms,” IEEE Trans. Neural Networks, vol. 12, Iss. 2, pp. 181–201. Mar. 2001.